encit 2020

ABCM
Associação Brasileira de Engenharia e Ciências Mecânicas

18th Brazilian Congress of Thermal Sciences and Engineering
November 16–20, 2020 (Online)

ENC-2020- MODELING A THERMOACOUSTIC ENGINE UNDER ROTT'S APPROACH FROM EXPERIMENTAL TRANSFER MATRICES OF A THERMOACOUSTIC CORE

Bárbara Alves Pereira de Carvalho Ferro
University of Campinas (UNICAMP), School of Mechanical Engineering, Campinas, Brazil
barbara_cv_ferro@hotmail.com

Flávio de Campos Bannwart
University of Campinas (UNICAMP), School of Mechanical Engineering, Campinas, Brazil
fcbannwart@fem.unicamp.br

Abstract. *The thermoacoustic engine onsets due to the spontaneous thermoviscous interaction between an acoustic particle and the surface of a solid substrate, ignited when the latter is submitted to a sufficiently high temperature gradient along the direction of acoustic propagation within a waveguide. This effect, namely thermoacoustic, consists in a conversion of thermal into acoustic energy, whose magnitude is proportional to the area of exposition for the interaction, besides other factors. In this way, the porous material in the thermoacoustic core (TAC) is a key point within the engine as it increases the total available area, provided by the pore internal walls. This study consists in a simulation and analysis of a previously conceived and experimentally characterized thermoacoustic engine in the transfer matrix context, from another work, in the free software DeltaEC environment -under Rott's approach context. Once the simulated model matches the real engine, we expect to disclosure variables that until then were hidden in the original data within the measured transfer matrices of the thermoacoustic core (T_{TAC}), such as the temperature profile along the device, heat and acoustic power, among others. So far, we have reached some degree of approximation. In the sequence, the goal of this investigation is to enable the editing of variables in the simulation and even in the transfer matrix itself, deliberately changing its coefficients. Based on the arbitrary performance of the engine, this altered T_{TAC} may indicate corresponding changes, via inverse problem, in the porous material such as geometric parameters or thermophysical properties. Therefore, the resulting model may be a tool to potentially improve the performance of real systems in the stage of design.*

Keywords: *thermoacoustics, transfer matrix, acoustic power, inverse problem*

1. INTRODUCTION

Thermoacoustics is an subject of acoustics that studies the conversion of thermal into mechanical energy and vice-versa by means of the thermoacoustic effect, which appears spontaneously under special conditions. Whenever a gas parcel (or acoustic particle) contained in a resonant chamber is in thermoviscous contact with a solid surface under sufficiently high temperature gradient, spontaneous acoustic oscillations are triggered, and a thermoacoustic engine is thus formed; the other way around, when a sufficiently intense acoustic field is imposed by external means in such environment, a temperature gradient appears along the solid surface because of the thermoacoustic heat pumping from the increasingly low temperature regions to the hotter counterpart. *"The thermoacoustic processes comprise the interactions between displacement, pressure, density, and temperature oscillations of an acoustic wave in a compressible fluid in thermoviscous coupling with a immobile surface acting as a thermal reservoir"* (Hayden and Swift, 1997).

For engines, the thermoacoustic effect consists in another heat transfer pathway, besides conduction, convection and radiation, driven toward the thermal equilibrium, whose consequence is the acoustic field generation. Its outbreak, however, demand the thermal potential to overcome the intrinsic thermal and viscous losses, so that to lead the gas parcel to follow a combined cycle of compression and expansion along its displacement close to the solid surface. Depending on acoustic waveguide configuration, either Brayton or Stirling cycle can be approached (Swift, 1988).

Compared to equivalent conventional devices, the thermoacoustic engines are around 25% less efficient, but, because of their single phase working fluid, they are more capable to perform low grade energy regeneration. This key aspect justifies much of the effort on the development of those devices, besides their higher reliability due to the absence of movable parts. Two main objetives are usually considered: either improving the thermal efficiency or reducing the thermal potential required to onset the thermoacoustic effect, and therefore regenerate low quality thermal energy into an acoustic form, which ends up resulting in electric energy by means of a proper acoustic pressure transducer (Swift,

2000). Together with its constructive simplicity, thermoacoustic engines are still seen to have potential of advantageous use in specific applications (Kruse *et al.*, 2017; Alcock *et al.*, 2018).

The thermoacoustic effect is magnified in the direct proportion with the area of exposition of the solid surface involved, besides the thermal potential. That is why the porous material is the key element of a thermoacoustic device, as it provides additional surface from the pore internal walls and is capable to ensure a high temperature difference between its ends. The thermoacoustic porous materials may be classified in two main kinds: stack or regenerator, in respective accordance with standing wave or traveling wave devices. When it comes to both thermal efficiency and acoustic power, factors such as porous geometry, stack or regenerator porosity, temperature profile and operating conditions of the working fluid are directly determinant. In this work, a previously conceived thermoacoustic engine obtained from experimental transfer matrices is investigated towards its implementation in a simulation software for thermoacoustic systems called Design Environment for Low Amplitude ThermoAcoustic Energy Conversion, commonly known as DeltaEC. This software proceeds a numerical integration in one spatial dimension using a low-amplitude acoustic approximation and sinusoidal time dependence (Ward *et al.*, 2016). It integrates the Rott's wave equation (Rott, 1980) in a gas to a given geometry using the trigger method. The method in turn analyzes several parameters to satisfy a variety of boundary conditions imposed, which gives the user greater flexibility in choosing the variables that will be system solutions. Once an equivalent model is achieved in the DeltaEC environment, we expect to unveil several variables whose values are hidden in the original experimental transfer matrices data, such as the temperature profile along the porous material, for example. As a result, the possibilities of achieving new solutions from this previous experimental basis may be amplified, as variables can be edited directly in simulations.

Following the goal of higher efficiencies and capacity of low grade energy regeneration, the purpose of this investigation is to enable those gains by, at first, distinguishing features that may cause or not such effects. Some of them are directly related to the temperature profile imposed by external conditions, while others are in great measure consequence of geometric features of the porous materials. Once minimally distinguished, then they may be easily edited in the DeltaEC simulations. One way to interfere is to directly edit the coefficients of the transfer matrices, as a continuation of the work developed by Gomes and Bannwart (2018). The latter consists in the synthesis of the transfer matrix of a thermoacoustic core, departing from experimental data of the same previous works utilized here (Bannwart, 2014; Bannwart *et al.*, 2013), aiming to achieve better performance in a thermoacoustic engine simulated using the transfer matrix method; the preliminary goal was achieved, however the causes for that were not distinguished on how important was the contribution of the input heat power, instead of an actual better machine. We expect in this work to contribute in this enlightenment so that to improve the choice of porous materials to conceive better performing thermoacoustic engines.

2. DELTAEC MODELING

For the computational modeling of the work, a standing wave thermoacoustic engine configuration is selected from the previous work of (Bannwart, 2014), whose operating characteristics resulted close to the highest gain and performance for the specific porous material case. This engine is constituted by a thermoacoustic core (TAC) and its surrounding waveguides with length $L_1 = 1.292m$ and $L_2 = 53.8mm$, both with cylindrical cross section and an internal diameter of $33.9mm$. The porous material is a Ceramic Catalyst (CCat) of length $74mm$.

The thermoacoustic core utilized in this work, Fig. 1, which is generally defined as the waveguide section of non-homogeneous temperature profile, is internally constituted by a porous material (stack) and three heat exchangers. Its active part is delimited by the left cold heat exchanger (AHX) and the hot heat exchanger (HHX), while the porous material in between them, while the passive part constitutes the interval between the the HHX and the right AHX. It is assumed that the gas temperature is homogeneous throughout the cross section, however, within the TAC, the profile is unknown so far. It can be expected, as an approximation, a continuous curve linking the heat exchanger regions, working in steady state regime. The engine geometry is kept unchanged to keep the model as close as possible to the experimental one.

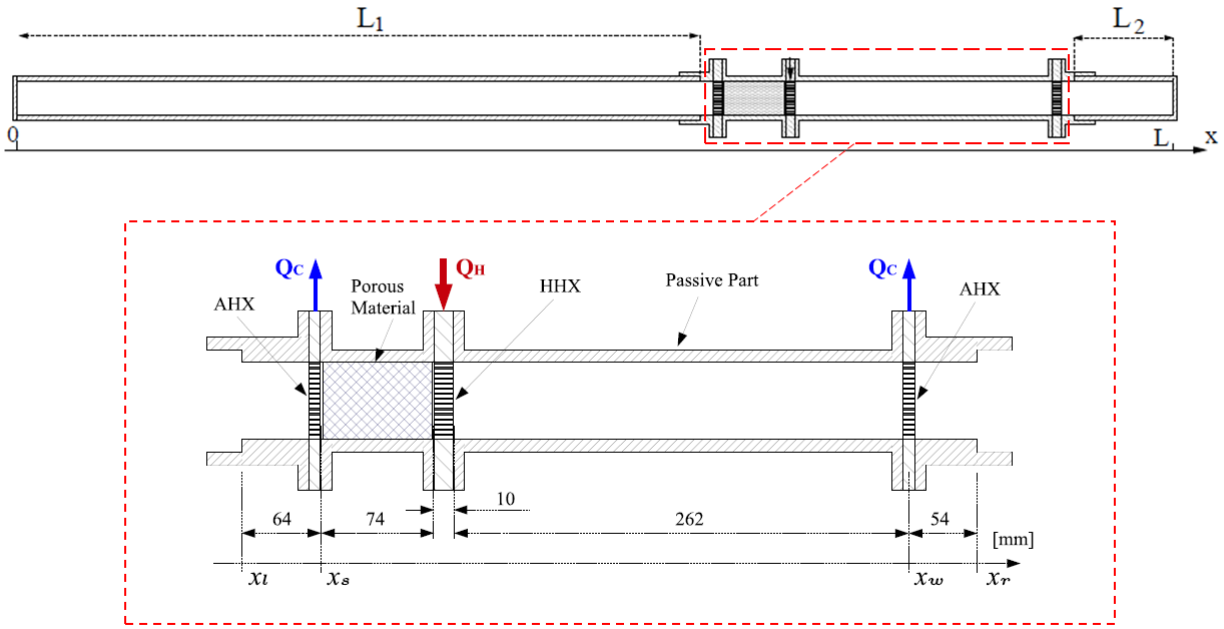

Figure 1. Schematic representation of the standing wave engine. Extracted from Bannwart (2014).

The first stage of modeling begins by projecting into the software the representation of all parts of the experimental device, used as reference. When defining the porous material, the software did not present in its scale of materials one that was similar of what had been used in the experimental work, so there was a need to choose another element. As a resuk, the simulated porous material and the whole device were defined based on the greatest similarity of geometrical and thermophysical properties so far.

The main segments required for modeling are: BEGIN, SURFACE, ANCHOR, DUCT, TX, STKRECT, STKDUCT, HARDEND and RPN. The TX represents a Tube-array heat exchanger with the thermoacoustic working gas passing through the tubes, while the ANCHOR is placed to change the standard thermal insulation of the segments, for a system that considers it as if they were immersed in a thermal bath. STKRECT is used to model cells of standing wave thermoacoustic motors with rectangular pores and STKDUCT functions as a pulse tube. As the thermoacoustic system is closed, the HARDEND segment is used. RPN allows you to create non-standard assumptions, targets and simple algebraic calculations anywhere in the DeltaEC model.

Figure 2. Simulated model in DeltaEC.

In the BEGIN section, the average operating pressure is set at $101.900kPa$, the fluid inlet temperature at $295.1K$, the pressure range is $1Pa$ with a phase angle of $0°$, the volume flow rate the amplitude is $9.8579e-08m^3/s$ with phase $178.25°$ and the working fluid is air. According to Swift (2003), the acoustic power depends strongly on the phase angle between $\tilde{p}$ and $\tilde{U}$, thus, the fact that none of these components is null is what allows the presence of acoustic power in the engine. Finally, it is determined that the operating frequency is an estimate in the calculations.

The materials chosen to compose the STKRECT and TX segments are stainless steel and copper, respectively, and for the other segments they are adopted as the ideal material. In the hot heat exchanger and the cold heat exchanger of the passive part, the sandy porosity is fixed at 1 and for the cold heat exchanger of the active part, the porosity is fixed at 0.9.

The porosity determined in the stack is 0.83 and in the RPN segment the value of $0.7583m^3/s$ for the pressure range in the DUCT is imposed as a target. It is defined that the heat that enters the cold HX of the active part is a guess and that

this value is automatically replicated in the cold HX of the passive part, in order to facilitate the modeling of the engine. Likewise, for hot HX, a guess is given for the heat supplied to the system. As it is a closed system, the volume flow rate amplitude at the right end of the model tends to zero. To qualify this imposition, two targets are added in the HARDEND segment that determine that the real part of the inverse of the specific normalized impedance and the imaginary part are zero.

3. TRANSFER MATRIX

The use of a transfer matrix T allows a simplified approach in modeling the sound propagation in resonators. In general, it is a well used resource due to the difficult fluid-dynamic description in porous materials. Once determined, in our case obtained from measurements of the aforementioned previous work, it is possible to know the acoustic field throughout the equipment at any point on the device excepting the TAC, treated as a *black box*. The model is divided into three segments, one for the TAC and the other two for the straight and cylindrical waveguides that make up the thermoacoustic engine (TAE), of which each has a sequential matrix with four coefficients.

3.1 Matrix T of waveguides

The acoustic propagation in a waveguide is determined analytically, according to linear plane wave acoustics for homogeneous temperature profile, as

$$T_w = \begin{bmatrix} cos(kL_w) & iZ_c sin(kL_w) \\ \frac{i}{Z_c} sin(kL_w) & cos(kL_w) \end{bmatrix}, \tag{1}$$

where, w refers to the L_w length waveguide. The complex wave number k counts for the losses that occur on the internal walls of the guides through the thermoviscous losses, being characterized as:

$$k = k_0 \sqrt{1 + \frac{f_v + (\gamma - 1) f_k}{1 - f_v}}, \tag{2}$$

where f_v and f_k are viscous and thermal loss functions, γ is the ratio of specific heats and $k_0 = w/c_0$ is the wave number. The complex characteristic impedance, Z_c, of the duct is given by:

$$Z_c = \frac{\rho_0 c_0}{\phi S \sqrt{(1 - f_v)[1 + (\gamma - 1) f_k}}, \tag{3}$$

ρ_o being the density of the fluid at room temperature T_0, ϕ the porosity of the material, S the cross-sectional area of the material. Thus, the transfer matrices T_1 and T_2 allow the determination of the acoustic field $\left\{\tilde{p}\tilde{U}\right\}^T$ at the exit of your segment from of your entry, as described in the following equations

$$\begin{Bmatrix} \tilde{p_l} \\ \tilde{U_l} \end{Bmatrix} = T_{1(w)} \cdot \begin{Bmatrix} \tilde{p_0} \\ \tilde{U_0} \end{Bmatrix} \tag{4}$$

and

$$\begin{Bmatrix} \tilde{p_L} \\ \tilde{U_L} \end{Bmatrix} = T_{2(w)} \cdot \begin{Bmatrix} \tilde{p_r} \\ \tilde{U_r} \end{Bmatrix}, \tag{5}$$

that describe the acoustic wave propagation from the entrance L_1, $\left\{\tilde{p_0}\tilde{U_0}\right\}^T$, until the exit, $\left\{\tilde{p_l}\tilde{U_l}\right\}^T$, the same way for the waveguide L_2.

3.2 TAC Matrix T

The experimental T_{TAC} had been measured as function of angular frequency (w) and heating power ($\dot{Q}_H$). From (Bannwart *et al.*, 2013):

$$\begin{Bmatrix} \tilde{p_r} \\ \tilde{U_r} \end{Bmatrix} = T_{TAC(w,\dot{Q}_H)} \cdot \begin{Bmatrix} \tilde{p_l} \\ \tilde{U_l} \end{Bmatrix} = \begin{bmatrix} T_{pp} & T_{pu} \\ T_{up} & T_{uu} \end{bmatrix} \cdot \begin{Bmatrix} \tilde{p_l} \\ \tilde{U_l} \end{Bmatrix}, \tag{6}$$

where the coefficients T_{pp}, T_{pu}, T_{up} and T_{uu} depend on the frequency of operation and the temperature distribution, to be uncovered. Together, they form a set that establishes a connection between the pressure and volume velocity of the input acoustic field with the pressure and volume velocity of the output.

4. Results and discussion

In this section, the results of the implementation of the real engine in DeltaEC are presented. The value of the heat flow removed from the HHX is estimated along with the average engine profiles. The complex pressure $\tilde{p}(x)$, the volume velocity $\tilde{U}(x)$ and the acoustic power are represented in Fig. 3. The acoustic pressure peaks at the tips of the engine and the volume velocity starts to increase from the stack, as expected. Meanwhile, it is observed that the acoustic power is initially negative and this is due to the configuration in the DeltaEC modeling. For the software convention, the positive acoustic power correspond to cooling systems, and the negative one for engines; therefore, in our case, a negative value is expected for this variable.

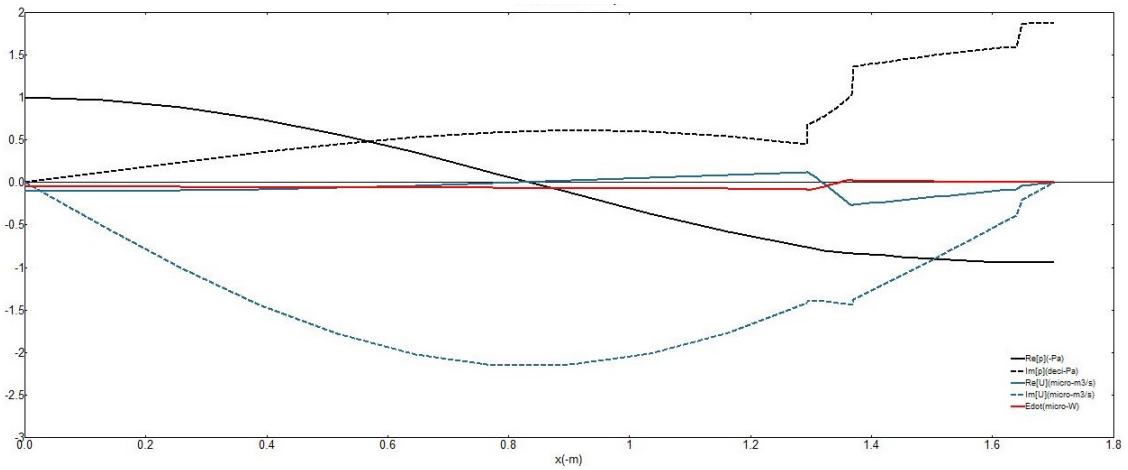

Figure 3. Real and imaginary volume velocity, real and imaginary acoustic pressure and acoustic power.

Figure 4 shows the temperature profile in the longitudinal direction x of the working fluid and of the solid surfaces, which are very close, except in the regions of the hear exchanger; the acoustic power and the total power produced are also revealed. The inhomogeneous temperature profile is observed in the porous material and in the passive part of the thermoacoustic core, as expected.

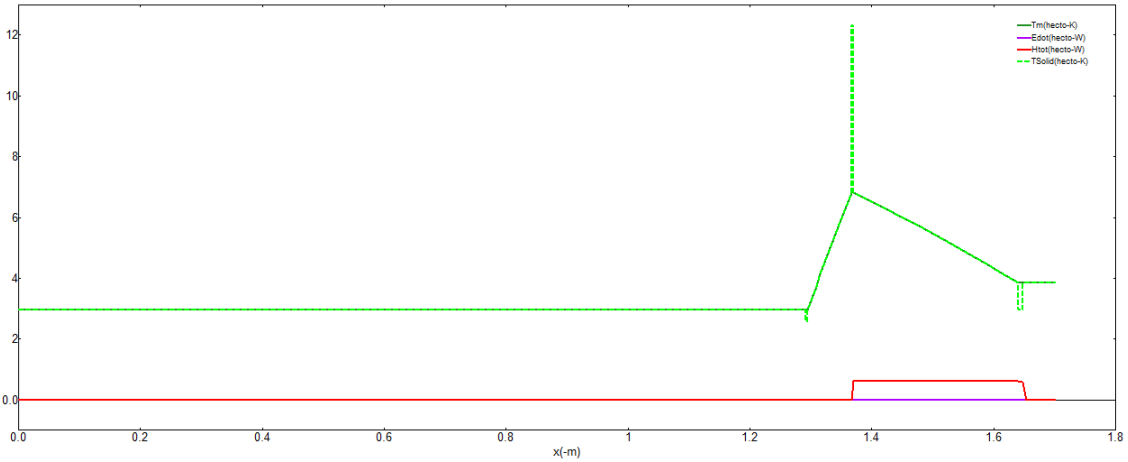

Figure 4. Temperature profile of the working fluid in the direction x, temperature profile of the solid, acoustic power and total power produced.

We also verified that the acoustic power produced in the core is negative (Fig. 5), as expected from a DeltaEC convention, and that the temperature decreases from the region of the hot TX in both directions, along the stack and along the passive part of the thermoacoustic core, as expected; such behavior is ensured by the three heat exchangers. For this engine, still under investigation, it is noticeable that a significant part of the acoustic power generated at the left end of the stack is dissipated by irreversible losses of viscosity and thermal relaxation within the left waveguide, and hence along the

entire resonator. Such a high proportion may be related to low average acoustic pressure of the experiment, established this way according to the purposes of that investigation. An addendum to the total power is that, according to Swift (2003), it cannot depend on x inside a stack or regenerator, having it to be constant regardless of x, although the acoustic power depends heavily on x.

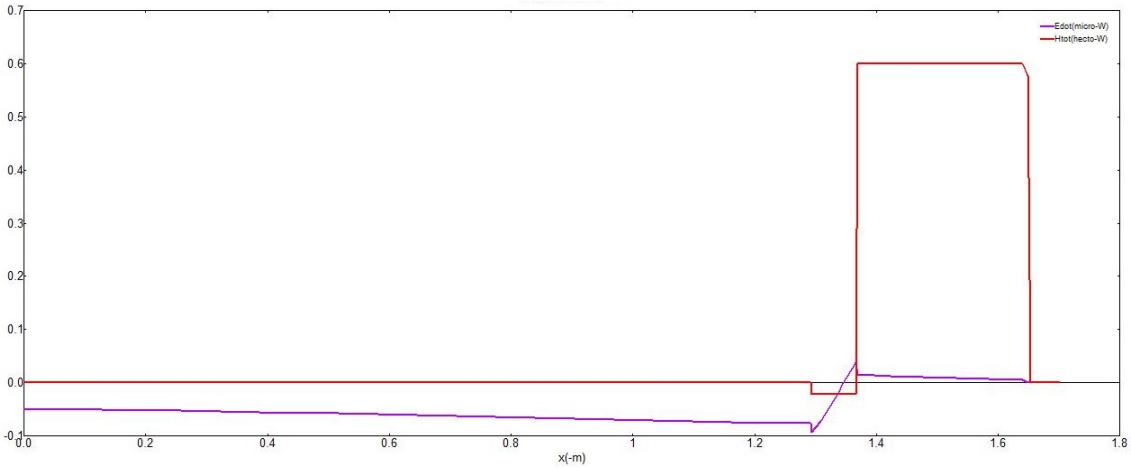

Figure 5. The acoustic power and the total power produced.

The frequency of operation in BEGIN was imposed as a guess, for which was expected the value of $102.2Hz$. This frequency was used to calculate the acoustic fields in the transfer matrices. After the simulation, the guess's response frequency was $102.11Hz$, hence very close. Another calculated guess was the heat entering the heat exchangers, with $-2.1938W$ in the cold TX and $62.107W$ in the hot TX. The original value used in the experiment for the heat inserted by the hot heat exchanger was $81W$. However, heat leakage to the environment was important and those losses were not accounted nor relevant for that investigation (see Bannwart (2014)); therefore, the thermal power actually transferred to the working fluid was surely lower. That said, the value found for the present estimate is consistent.

In the experiment, the temperature of the water circulating in the cold heat exchangers was $295.15K$. To facilitate the present computational modeling, we assume that the temperature of the solid in the cold heat exchangers is close to the water temperature. In the cold TX of the passive part, the temperature of the solid reached $295.97K$ after the simulation, and in the active part reached $256.05K$.

The acoustic fields for the imposed conditions were extracted from the experimental transfer matrices, and they are shown in Tab. 1, together with the DeltaEC results. It is important to note that the values extracted from the matrices were adjusted for the convection ($+i\omega t$), adopted in the DeltaEC convention.

Table 1. Acoustic fields calculated by transfer matrices and by DeltaEC. Expected acoustic field extracted from measurements of Bannwart (2014).

Segment	Expected acoustic field		DeltaEC acoustic field	
	Module	Phase (deg)	Module	Phase (deg)
$\tilde{p}_0$ $[Pa]$	1	0	1	0
$\tilde{U}_0$ $[m^3/s]$	9.8579e-08	178.2447	9.8579e-08	178.25
$\tilde{p}_l$ $[Pa]$	0.7583	176.5980	0.7583	176.60
$\tilde{U}_l$ $[m^3/s]$	1.4183e-06	-85.2646	1.4195e-06	-85.256
$\tilde{p}_r$ $[Pa]$	1.2098	167.8606	0.9577	168.79
$\tilde{U}_r$ $[m^3/s]$	2.6525e-07	-102.4915	2.1029e-07	-101.66
$\tilde{p}_L$ $[Pa]$	1.2160	167.8565	0.9615	168.78
$\tilde{U}_L$ $[m^3/s]$	2.3210e-22	-87.7400	6.9251e-21	-173.20

The input values were imposed on BEGIN, with the pressure amplitude at the left end of the nucleus by the RPN. The other results were generated automatically by the composition of the model. It is possible to notice that the volume velocity in "x_l" returned a similar value to that calculated by the matrices.As it is a closed system, there is a rigid wall in the position "x_L" where "U_L" is zero, that is, the values of the modules in that segment resulting from DeltaEC, by numerical convergence, are zero. The other segments were close enough to the expected values to be considered valid.

The disparity found may be related to the unknown values that were assumed within TX's, STKRECT and STKDUCT. For example, the porous material inside the nucleus is not the same as in the experiment, but the one that had the greatest

similarity within the options offered by DeltaEC. The same happens with the type of heat exchanger used experimentally and the one adapted in the simulated version. These adaptations may be reflecting the differences found in the pressure ranges and volume velocities.

5. CONCLUSIONS

In this work, we propose to perform the equivalent of a real thermoacoustic engine modeled in the DeltaEC thermoacoustic software. This simulation allows the visualization of parameters that are not explicit in the T_{TAC} measured in previous works. From them, it is possible to extend the analysis and exploration toward other variables and features through the same experimental base and, possibly, to enable the transfer matrix coefficients to be edited consistently and reliably.

The results of this approximate equivalence between the two system are promising, but they still need to be adjusted and refined to obtain greater equivalence. The operating frequency between the two models showed a difference of less than 1%. The temperatures of the solid surfaces in the heat exchangers of the active and passive parts are surely higher than in the actual experiment, but are not unrealistic. The heat power of entry into the hot TX is significantly less than $81W$, which was expected mainly due to the heat losses of the experiment.

The acoustic fields shows small differences in most results for the four positions evaluated. The biggest variations are found after the thermoacoustic core, which are of around 20.8% for acoustic pressure and 20.7% for volume velocity in "x_r", both in amplitudes; similar variation is found in "x_L", also for acoustic pressure amplitude. This disparity may be related to the lack of choices for porous materials and to the limitation in the models of heat exchangers and chimneys provided by the software.

As a continuation of this work, the model can be adjusted by varying the heat exchangers and the stack, in order to evaluate the behavior of the acoustic fields and their similarity with the experimental characterization. Once a greater correspondence is achieved, a more accurate investigation can be proceeded.

6. REFERENCES

Alcock, A.C., Tartibu, L.K. and Jen, T.C., 2018. "Experimental investigation of an adjustable standing wave thermoacoustic engine". *Heat and Mass Transfer*, pp. 206–2018.

Bannwart, F., 2014. *Methods for the transfer matrix evaluation of thermoacoustic cores with application to the design of thermoacoustic engines*. Ph.D. thesis, Ph. D. thesis, Université du Maine/Unicamp.

Bannwart, F., Penelet, G., Lotton, P. and Dalmont, J.P., 2013. "Measurements of the impedance matrix of a thermoacoustic core: Applications to the design of thermoacoustic engines". Vol. 133, pp. 2650–2660. doi:10.1121/1.4796131.

Gomes, D. and Bannwart, F., 2018. "On the synthesis of the transfer matrix of thermoacoustic cores from arbitrary engine performance". doi:10.26678/ABCM.ENCIT2018.CIT18-0656.

Hayden, M. and Swift, G., 1997. "Thermoacoustic relaxation in a pin-array stack". *The Journal of the Acoustical Society of America*, Vol. 102, No. 5, pp. 2714–2722.

Kruse, A., Ruziewicz, A., Tajmar, M. and Gnutek, Z., 2017. "A numerical study of a looped-tube thermoacoustic engine with a single-stage for utilization of low-grade heat". *Energy Conversion and Management*, Vol. 149, pp. 206–2018.

Rott, N., 1980. "Thermoacoustics". *Advances in Applied Mechanics*, Vol. 20, No. C, pp. 135–175.

Swift, G.W., 1988. "Thermoacoustic engines". *The Journal of the Acoustical Society of America*, Vol. 84, No. 4, pp. 1145–1180.

Swift, G.W., 2000. "Thermoacoustic engines and refrigerators". Vol. 524. doi:10.1063/1.1309184.

Swift, G.W., 2003. "Thermoacoustics: A unifying perspective for some engines and refrigerators".

Ward, B., Clark, J. and Swift, G., 2016. "Design environment for low-amplitude thermoacoustic energy conversion, deltaec version 6.4 b2 users guide". *Los Alamos National Laboratory Network*.

7. RESPONSIBILITY NOTICE

The authors are solely responsible for the printed material included in this paper.